

Tracking Multiple Dynamic Targets in LoS-NLoS Condition with Multidimensional Scaling

Davide Macagnano and Giuseppe Thadeu Freitas de Abreu
 Centre for Wireless Communications - University of Oulu
 P.O.Box 4500, 90014-Finland
 [macagnan,giuseppe]@ee.oulu.fi

Abstract—We consider the problem of tracking multiple targets in the presence of noise and a mixture of line-of-sight (LoS) and non-line-of-sight (NLoS) conditions. The targets are assumed to describe independent trajectories with non-stationary (dynamic) statistics, *i.e.*, with variable velocities and accelerations (limited in absolute value). These moving targets are observed by fixed anchors, which measure the distance between themselves and each target periodically. LoS and NLoS conditions are modeled by a first order time-homogeneous Markov chain, such that the occurrence, the intensity and the persistence (duration) of transitions between LoS and NLoS states are random but according to the steady state distribution of the process. The challenge, therefore, is that such variations are difficult to detect in the presence of noise and target mobility, and if not corrected, may result in severe degradation of tracking accuracy. In order to mitigate this problem we introduce a wavelet-based technique to simultaneously attenuate the noise effect on ranging and detect the LoS-NLoS transitions, allowing for their subsequent correction. The technique is non-parametric, in which no knowledge of the statistics of the LoS/NLoS transition process is assumed. The impact of such pre-filtering on the performance of the Multidimensional Scaling (MDS) tracking algorithm (proposed in an earlier work) is studied, and for the LoS case compared against the error performance for classic Extended Kalman Filter (EKF). It is shown that the MDS-based tracking algorithm with Jacobian eigenspace updating together with wavelet pre-filtering is superior (at the region of interest) to the EKF approach, and can well cope with mixed LoS-NLoS scenarios.

I. INTRODUCTION

Sensor mobility is a topic of growing interest in wireless sensor networks (WSNs). Although many traditional sensor network application scenarios tend to be static, mobility finds itself at the heart of several new system concepts and techniques for WSNs. The combination of mobility as a feature, and localization as a need or application, gives rise to the problem of target tracking in sensor networks, which is subjected to distinct challenges to those met in more traditional contexts such as array antennas, radar or GPS technology. Specific difficulties vary with the application, but some of the major challenges for tracking algorithms in the WSN context are stringent constraints on the power consumption of sensors activated for tracking purposes [1], the requirement for low-complexity algorithms [2], the ability to track a potentially large number of sensors simultaneously [3] as well as robustness to different target dynamics [4].

Having this in mind and aiming at centralized applications, *e.g.* warehouse logistics or surveillance systems, we consider

a scenario where a small number of inter-wired anchor nodes placed at known fixed locations provide the infra-structure used to perform ranging, *i.e.*, collect all anchor-to-target time of arrivals (TOAs). The challenges with tracking multiple dynamic targets in the scenario described above are related to the number of mobile targets to be simultaneously tracked, *i.e.* the computational complexity of the system and the ability to cope with the different target dynamics simultaneously [4].

As far as ranging is concerned, ultra wide band (UWB) is one promising technology for indoor applications thanks to its sub-centimeter resolution, the ability to minimize interference to other services and its penetration properties through different material. However, links between tags and anchors may be in line-of-sight (LoS) or non-line-of-sight (NLoS), which affects the quality of range measurements. Particularly at indoor environments, where a large number of objects and scatterers are closely spaced, the NLoS conditions cause ranging to be performed over reflected signals, with the introduction of biases (positive increments) on the estimated distances. Consequently it is essential to use tracking algorithms that, while capable of coping with a wide range of target dynamics, can still infer and mitigate the presence of such errors/biases directly from the observation, all without introducing excessive delay (lag) on the location estimates.

In this paper, we propose an extension of the classic multidimensional-scaling (CMDS)-based tracking algorithm introduced in [5], improving its accuracy in the presence of noise and LoS-NLoS state transitions, with little effect on its complexity and robustness to variable target dynamics. This is achieved applying a wavelet smoothing filter (WSF) to the range estimates collected at the anchor nodes. The WSF technique employed [6] was chosen due to its fast response to sudden transitions on the measurements, its ability to characterize the type of transition itself, meaning the ability to distinguish between bias and noise, and its low complexity. In addition, since it exploits the signal properties at different scales, it can be used as a smoothing filter. The reminder of this article is as follows. In section II the ranging models and the Markov chain used to simulate the LoS-NLoS transitions are described. In section III, a brief description of the WSF properties and a description of its usage into the CMDS are presented. In section IV the CMDS-based tracking technique is revised, and in section V the error performance for the WSF as a smoothing filter, as well as its ability to detect and

mitigate LoS-NLoS transitions are investigated. The results indicate that the eigenspace-based CMDS tracking algorithm combined with the WSF is suitable to track a large number of devices simultaneously under mixed LoS-NLoS conditions.

II. RANGING MODEL

UWB-TOA-based ranging in indoor environments is subject to multipath and attenuation introduced by the obstacles. Consequently, depending on presence of LoS or NLoS between transmitter and receiver, different ranging performance can be expected. In other words, different ranging models apply depending on the state of the channel. As suggested in [7], we assume the range between devices i and j under LoS condition to be distributed accordingly to a $\Gamma(\alpha, \beta)$, as

$$\tilde{d} = \Gamma(\alpha, \beta) \quad \begin{cases} \alpha = \mu^2 \sigma^2 \\ \beta = \sigma^2 / \mu \end{cases}, \quad (1)$$

where σ^2 and μ denote the variance and the average value of the range measurement between the devices i and j . In our case, since only one range per sampling time is assumed, μ corresponds to the range measurement between $i - j$. Conversely, a NLoS channel occurs if the signal traveling on the direct path is more attenuated than another traveling in an indirect path, such that the traveling time is increased proportionally to the deviation, which leads to

$$\tilde{d}_b = \Gamma(\alpha_b, \beta_b) \quad \begin{cases} \alpha = \mu_b^2 \sigma^2 \\ \beta = \sigma^2 / \mu_b \end{cases}, \quad (2)$$

where σ^2 is still the variance for the noise process affecting the measurements, while μ_b is defined as $\mu_b = \mu + b$, where b accounts for the bias introduced estimating the range over an indirect path. In our simulation b is generated as a random process uniformly distributed between [4 – 7] meters. In order to combine the models described above and emulate the dynamic LoS-NLoS transitions observed in real scenarios, we follow what was proposed in [8], albeit with a slight modification. While in [8], the channel states are characterized by three different types of propagation paths, namely, the Detected Direct Paths (DDP), the Natural Undetected Path (NUDP) and the Shadowed UDP (SUDP), here we employ a simplified version of that idea, considering only two states (LoS and NLoS), with a random bias at each NLoS state occurrence. Since a transition from LoS to NLoS (or vice-versa) clearly does not depend on a target's previous locations, we model such transitions by a first-order time-homogeneous Markov chain, as illustrated in figure 1. The values for state transition matrix Π defining the Markov process, are fixed to 0.983 for p_1 and 0.965 for p_2 . Thus, using the convergence properties of time-homogeneous Markov chains, the steady state distribution of the process assumes a probability of 0.67 for the LoS state, and 0.33 for the NLoS state, with an average duration of 59 and 28 time-steps respectively.

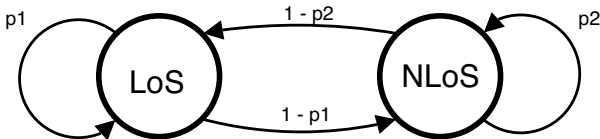


Fig. 1. 2 states Markov process used to model the LoS-NLoS state transition characterizing the ranging process.

III. NLOS DETECTION AND MITIGATION

Fourier analysis has been used, for a long time, as the main tool to study signal singularity, although while providing complete frequency information, due to its global supports, it does not include any temporal information. In fact, defining the time resolution as Δt , and the frequency resolution as Δf , the Heisenberg's uncertainty principle imposes $\Delta t \cdot \Delta f \leq 1/4\pi$.

One solution until recently used to overcome the shortcomings of Fourier Transform, was the Short Time Fourier Transform (STFT) [9]- [10], whose main limitation in studying time varying processes is the fixed time-frequency resolution imposed by the cutting window used in its computation.

A somewhat recent solution to overcome the shortcomings of Fourier expansions is the wavelet transform WT [10], which is able to characterize local regularity of signals using their decomposing into elementary blocks, well localized in both time and frequency [9]- [11]. In the following we give a brief introduction of the idea behind the wavelet-transform we use, for a detailed description of its properties and numerical implementation, please refer to [10]- [11].

A. Wavelet Transform Properties

The wavelet transform for a signal $f(x)$, corresponds to its decomposition into a set of frequency channels of the same bandwidth on a logarithmic scale.

This decomposition is done using the family of functions $\sqrt{s}\psi(s(x-u))_{(s,u) \in \mathbb{R}^2}$, corresponding to the translated and dilated version of the function $\psi(x)$, called wavelet, with s and u identifying the *scaling* and *translation* factors.

A result is that the function $\psi_s(x)$ is identical to $\psi(x)$, except for the size of its support, which is s times smaller.

As proved in [11], the Fourier transform of $\psi_s(x)$, here denoted by $\hat{\psi}_s(\omega)$, while $\hat{\psi}_s(\omega)$ being small enough in the neighborhood of $\omega = 0$, must satisfy $\hat{\psi}_s(0) = 0$, meaning that $\hat{\psi}_s(\omega)$ can be interpreted as a band pass filter.

Defining $\tilde{\psi}_s(x) \triangleq \psi_s(-x)$, and the continuous wavelet transform of $f(x)$ as

$$Wf(s, u) \triangleq \int f(x) \sqrt{s} \psi(s(x-u)) dx, \quad (3)$$

it is possible to look at $Wf(s, u)$ as the convolution computed at the point u , of $f(x)$ with $\tilde{\psi}_s(x-u)$ for the scale s , namely $Wf(s, u) = f(x) * \tilde{\psi}_s(x-u)$, which shows the band-pass filtering effect operated by $\psi(x)$ over $f(x)$.

Unlike the STFT, the WT decomposes the original signal $f(x)$ into a set of constant frequency bands on a logarithmic scale, Δt and Δf to change proportionally to the scale factor s , enabling the study of transient behaviors and irregularities in $f(x)$ through different scales [11].

The WT can be discretized sampling both s and u . Choosing the scale to be equal to $(\alpha^j)_{j \in \mathbb{Z}}$, with α as the elementary dilation step, then the necessity to sample uniformly at a rate proportional to α^j suggests the discrete dilation factor to be set equal to α^j / β [11], which defines the family of discrete wavelet functions $\psi_{\alpha^j}(x - n\beta/\alpha^j)_{(n,j) \in \mathbb{Z}^2}$.

In [10] it is shown that choosing $\alpha = 2$ and $\beta = 1$, the corresponding class of discrete dyadic wavelets $\psi_{2^j}(x - n/2^j)_{(n,j) \in \mathbb{Z}^2}$ constitutes an orthonormal basis (which also called orthonormal-wavelet).

This same class of wavelets has been used in [6] to characterize the local regularity of a signal $f(x)$ studying the approximation of its *Lipshitz* exponents. A generic function $f(x)$ is said to be α -Lipshitz in the neighborhood of x_0 , if and only if $\forall x$ close to x_0 there exists a K such that the following inequality is satisfied

$$|f(x) - f(x_0)| \leq K |x - x_0|^\alpha. \quad (4)$$

It is proved to be possible to check whether a $f(x)$ is α -Lipshitz in x_0 by looking at the decay of the wavelet coefficient in the neighborhood of x_0 [10]. In [6] the singularities of a function $f(x)$ are characterized through the study of Lipshitz exponents approximated by the wavelet transform at different scales. It shows the necessity to combine information at different scales in order to characterize the signal under investigation.

B. Wavelet Transform Application

As described in [6], to characterize the shape of irregular functions $f(x)$, the interest is towards wavelet defined as $\psi(x) = d\phi(x)/dx$, with $\phi(x)$ acting as a local average or smoothing function. Consequently the wavelet transform can be interpreted as derivative of a local average of $f(x)$, whose smoothing degree depends on the scale factor s as shown by

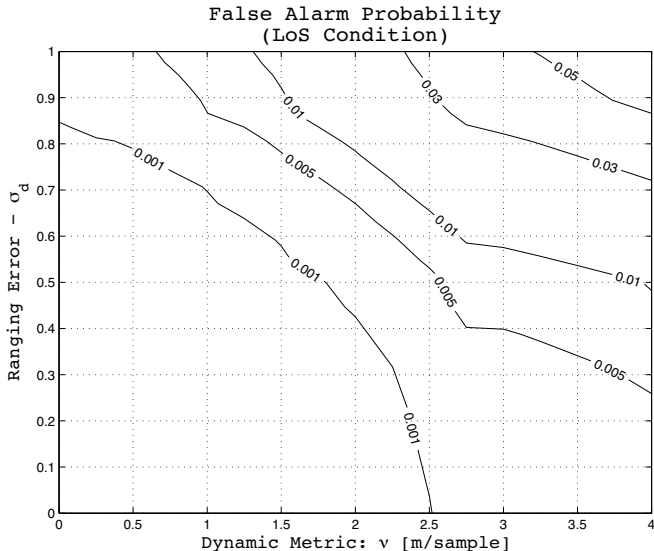
$$Wf_s(x) = f * \left(s \frac{d\phi_s}{dx} \right) (x) = s \frac{d}{dx} (f * \phi_s) (x). \quad (5)$$

Appendix A-B of [6] give the details to compute a fast implementation of a discrete dyadic wavelet transform, meaning $\psi(x)$ belonging to the family $\psi_{2^j}(x - n/2^j)_{(n,j) \in \mathbb{Z}^2}$, and whose coefficients $Wf(s, u)$ are used to approximate the Lipshitz exponents.

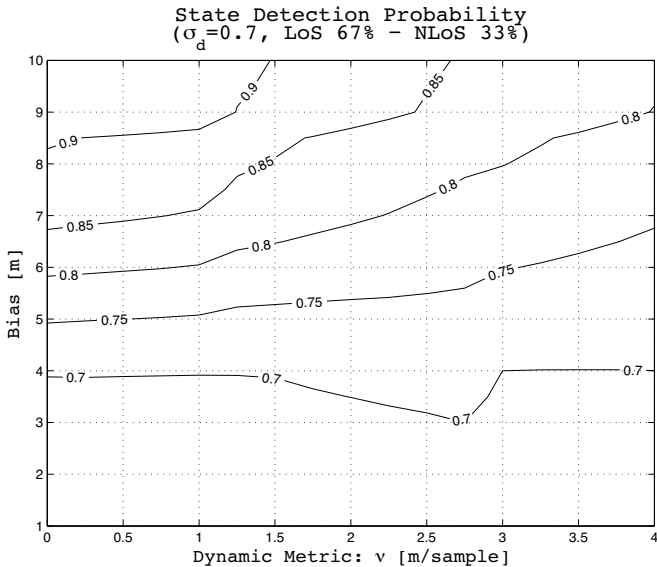
In our application the $f(x)$ corresponds to each one of the anchor-to-target time series $f(t)$, where t is sampling time, collecting the TOA range observation generated accordingly to equation (1)-(2), depending on the state of the channel at t . Trying to avoid the introduction of an excessive lag in the tracking system, we compute the wavelet transform described in [6] for $f(t)$ over a sliding window of 4 samples, where the first sample is the one for which we test the state condition. This corresponds to the introduction of a delay of 3 samples in the tracking system. Due to the size of the sliding window used, the scale parameter is fixed to 2.

In order to follow the evolution of the Lipshitz coefficients through the different scales, we exploit their correlation across the different scales computing a total index $W_T(t)$, defined as the product of the wavelet coefficients for the different s values. In addition, the coarse approximation of $f(t)$ at the scale 1 is used as smoothed (low-pass) version of $f(t)$.

$W_T(t)$ is used to detect-mitigate NLoS transition first testing whether it is a local maxima, accordingly to [6], then comparing its absolute value against a fixed threshold.



(a) False alarm probability under LoS condition as function of the dynamics \bar{v} and the measurement error σ_d .



(b) State detection probability under noisy measurements ($\sigma_d = 0.7$ [m]), as function \bar{v} and the bias.

Fig. 2. State detection probability for the WSF under both, pure LoS and mixed LoS-NLoS conditions as function of the dynamics \bar{v} , the measurement error ranging σ_d , and the bias affecting the NLoS measurements.

Due the scarcity of scales considered, and the perturbation effect introduced by the noise and the target dynamics \bar{v} over $f(t)$, the threshold mentioned above is set equal to 25.

Only for those t for which $W_T(t)$ satisfies the previous conditions, the occurrence of a state transitions is detected by checking $|f(t) - f(t + 1)| \geq B$, where B is an arbitrary threshold set equal to 3, in order to balance the different effects introduced by \bar{v} , σ_d^2 and the bias affecting $f(t)$ for the NLoS case. Accordingly to the sign of $|f(t) - f(t + 1)|$, we distinguish between LoS-to-NLoS and NLoS-to-LoS transition.

The compensation is computed every time that a LoS-

to-NLoS transition occurs, computing a the gap between $|f(t) - f(t+1)|$.

We call wavelet smoothing filter (WSF), the WT proposed in [6] together with the operations described above. The WSF performance to detect-mitigate NLoS states are shown in figure 2. Figure 2(a) provides the false alarm probability under LoS conditions, as function of the $\bar{\nu}$ and σ_d , while figure 2(b) shows, for $\sigma_d = 0.7$, the state detection probability for WSF under mixed LoS-NLoS condition, and as a function of $\bar{\nu}$ and the bias affecting the NLoS measurements. It can be noticed how the WSF allows to detect the state condition with high precision and with a very low false alarm probability.

IV. MDS-BASED TRACKING ALGORITHM

The CMDS-based tracking algorithm, first introduced in [5], does not rely on any model nor on more than the last estimate and current observations in order to update the estimates of the location of tracked target. Consequently, the performance results to be s is immune to the non-stationarity of the target's dynamics, although the complexity of the algorithm is not [4]. For the sake of clarity the structure of the MDS-based tracking algorithm proposed in [5] is here briefly reviewed. The algorithm is formulated over an incomplete Euclidean distance matrix (EDM) $\tilde{\mathbf{D}}$ which collects all the anchor-anchor \mathbf{D}_{A^2} and anchor-target distances $\tilde{\mathbf{D}}_{AM}(t)$ at each sampling instance.

$$\tilde{\mathbf{D}} = [d_{i,j}(t)] = \begin{bmatrix} \mathbf{D}_{A^2} & \tilde{\mathbf{D}}_{AM}(t) \\ \tilde{\mathbf{D}}_{AM}^T(t) & \mathbf{0} \end{bmatrix} \quad (6)$$

At any time t , the MDS techniques allows one to recover the location $\mathbf{Y}(t)$ of all sensors in the network (up to rotation, scaling, translation and reflection) from the complete Gram matrix $\mathbf{G}(t)$. Mathematically we have

$$\mathbf{Y}(t) = [\mathbf{V}(t)]_{1:n} \cdot [\mathbf{A}(t)]_{1:n}^{\frac{1}{2}}, \quad (7)$$

$$\mathbf{G}(t) = \mathbf{V}(t) \cdot \mathbf{A}(t) \cdot \mathbf{V}(t)^T, \quad (8)$$

where a complete Gram-matrix $\mathbf{G}(t)$ can be obtained from the incomplete $\tilde{\mathbf{D}}$ using the Nyström approximation [12],

$$\mathbf{G}(t) \approx \begin{bmatrix} \mathbf{G}_A & \mathbf{G}_M(t) \\ \mathbf{G}_M(t) & \mathbf{G}_M(t)^T \cdot \mathbf{G}_A^{-1} \cdot \mathbf{G}_M(t) \end{bmatrix}, \quad (9)$$

with [13],

$$\mathbf{G}_M(t) = -\frac{1}{2} \cdot \left(\tilde{\mathbf{D}}_{AM}(t) + \mathbf{C}_1 - \mathbf{C}_2 - \mathbf{C}_3(t) \right), \quad (10)$$

$$\mathbf{C}_1 = \frac{1}{A^2} \cdot \left[\mathbf{e}_{[1 \times A]} \cdot \mathbf{D}_{A^2} \cdot \mathbf{e}_{[A \times 1]} \right] \cdot \mathbf{e}_{[A \times M]}, \quad (11)$$

$$\mathbf{C}_2 = \frac{1}{A} \cdot \left[\mathbf{D}_{A^2} \cdot \mathbf{e}_{[A \times 1]} \right] \otimes \mathbf{e}_{[1 \times M]}, \quad (12)$$

$$\mathbf{C}_3(t) = \frac{1}{A} \cdot \left[\mathbf{e}_{[1 \times A]} \cdot \tilde{\mathbf{D}}_{AM}(t) \right] \otimes \mathbf{e}_{[A \times 1]}. \quad (13)$$

Provided that the coordinates $\mathbf{X}_A(t)$ of at least $A > n$ anchor nodes are known with respect to an absolute system of coordinates, the solution $\mathbf{Y}(t)$ can be re-oriented via the Procrustes transformation [14], returning $\hat{\mathbf{X}}(t)$.

As indicated by equation (7), tracking with the MDS algorithm requires the repetitive computation of eigen-decomposition of $\mathbf{G}(t)$. This problem can be circumvented by utilizing an iterative eigenspace adaptation technique based on the Jacobian algorithm [15], summarized by

$$\mathbf{A}_{k+1} \leftarrow \mathbf{R}(i_k, j_k, \theta_k) \cdot \mathbf{A}_k \cdot \mathbf{R}(i_k, j_k, \theta_k)^T, \quad (14)$$

where $\mathbf{R}(i_k, j_k, \theta_k)$ are orthogonal similarity transformations corresponding to the Givens rotation matrices, whose optimum rotation angle for the plane associated with the quartet $(a_{i,i}, a_{i,j}, a_{j,i}, a_{j,j})$ is given by,

$$\theta_{\text{Opt}}(i, j) = \frac{1}{2} \cdot \text{atan} \left(\frac{a_{i,j} + a_{j,i}}{a_{i,i} - a_{j,j}} \right). \quad (15)$$

In the Jacobian algorithm, the approximate eigenvector matrix of \mathbf{A} obtained after K_E iterations is given by,

$$\mathbf{V} = \prod_{k=1}^{K_E} \prod_{(i_k, j_k)} \mathbf{R}(i_k, j_k, \theta_k). \quad (16)$$

A Jacobian-like eigen-decomposition algorithm capable of finding a single matrix \mathbf{R} that jointly (approximately) diagonalizes a set of matrices $\mathcal{A} \triangleq \{\mathbf{A}_1, \dots, \mathbf{A}_M\}$ also exists [16].

In this Jacobian-like joint-diagonalization technique, one iterates the expression

$$\mathcal{A}_{k+1} = \mathbf{R}(i_k, j_k, \theta_k) \cdot \mathcal{A}_k \cdot \mathbf{R}(i_k, j_k, \theta_k)^T \quad (17)$$

where $\mathbf{R}(i_k, j_k, \theta_k)$ is the solution of

$$\min_{\theta(i,j)} \sum_{m=1}^M \text{off}(\mathbf{R}(i, j, \theta) \cdot \mathbf{A}_m \cdot \mathbf{R}(i, j, \theta)^T), \quad (18)$$

with

$$\text{off}(\mathbf{A}) \triangleq \sum_{i \neq j} \|a_{i,j}\|^2. \quad (19)$$

Convergence and stability of this algorithm are rigorously proved in [16]. In the form presented thereby, however, the algorithm would be too computationally demanding for our needs, due to the optimization step described by equation (18). Fortunately, closed-form expression for the optimum angles that solve this minimization problem was later discovered [17]. The solution thereby is extremely simple and are applicable for any set of equi-dimensional matrices \mathcal{A} , regardless of symmetry and commutativity properties. As noted in [5], the joint-diagonalization algorithm with closed-form optimum rotation angles can be used as an eigenspectrum tracking algorithm as follows. Consider the two Gram matrices $\mathbf{G}(t)$ and $\mathbf{G}(t+T)$ corresponding to consecutive observations $\tilde{\mathbf{D}}_{AM}(t)$ and $\tilde{\mathbf{D}}_{AM}(t+T)$, and assume that the eigenvector matrix $\mathbf{V}(t)$ of $\mathbf{G}(t)$ is known. Then, $\mathbf{V}(t+T)$ can be easily computed by initializing the Jacobian algorithm with $\mathbf{V}(t)$. This leads to the following solution for the eigen-decomposition of $\mathbf{G}(t+T)$,

$$\mathbf{V}(t+T) = \mathbf{V}(t) \cdot \prod_{k=1}^{K_E} \prod_{(i_k, j_k)} \mathbf{R}(i_k, j_k, \theta_k). \quad (20)$$

As proofed in [4], the number of iterations K_E required to update $\mathbf{V}(t)$ into $\mathbf{V}(t+T)$ will be related to the dynamics of the targets. For example, if the location of all targets at time $t+T$ differs only slightly from that at time t , it is fair to expect that K_E will be rather small. The conclusion that can be drawn is that K_E is not strongly dependent on ν implying that the complexity of the MDS-based algorithm is mainly determined by the number of targets and only slightly affected by the target dynamics.

V. COMPLEXITY AND PERFORMANCE

The scenario used to test the tracking algorithms, is a square in 2D space, with 20 meters long edges, and at whose corners find place the anchor nodes. The target trajectories are generated accordingly to a first order time homogeneous Markov process defined by $x(t) = x(t-1) + vt - 1$, where $v(t)$ is the 2D driving process corresponding to \bar{v} for the time t , and $x(t)$ the vector containing the trajectory coordinates at same time t .

A detailed account of the computational complexity and memory requirements of the CMDS and EKF tracking algorithms was performed in [5], while the target dynamics \bar{v} effect on the error performance for the above mentioned techniques was covered in [4].

Figures 3(a) repeats what already studied in [4] under LoS conditions, showing the error performance as function of the target dynamic \bar{v} for both the CMDS and the EKF tracking techniques. From this figure it is evident how the CMDS, being essentially a re-localization technique, except when provided with perfect ranging, performs poorly when the targets have slow dynamic. Differently, the EKF, thanks to the dynamic model incorporated in its prediction stage, is able to partially filter the noise affecting the range, making itself preferable to the CMDS technique under a pure error-performance point of view. Figure 3(b) shows the same result under noisy condition for the EKF compared against the error performance for the CMDS+WSF, when the WSF is used as smoothing filter. It is evident how the addition of the WSF as pre-filtering block improves the CMDS error performance up to high dynamics. Figure 4 shows the goodness of the smoothing (low-pass filtering) effect operated by the WSF on the range measurements. Nevertheless, once the target dynamic \bar{v} exceeds a certain value, both the smoothed and smoothed-corrected observations by the WSF degrade if compared to the measured distances.

However, it should be noted that, under the assumption of slow changes in the target dynamics, the same WSF could be employed, using a sufficient number of past observations, to estimate the slow-fast varying transients (time varying components) characterizing the measurements observations and related to the $\bar{v} - \sigma_d^2$. Consequently it should be possible to switch the WSF off accordingly to the $\bar{v} - \sigma_d^2$ estimated, allowing to match, in the case of high velocity, the CMDS error performance shown in figure 3(a). This is sustained by the false alarm probability illustrated in figure 2. As already stressed in I, the other important parameter that must be considered while evaluating multi-target tracking solutions, is the complexity.

Figure 5 compares the computational complexity of the CMDS+WSF-based tracking scheme against the one for the EKF, as a function of the number of targets. It is measured as the number of floating point operations (flops) incurred in the execution of the algorithm. It is evident that the CMDS+WSF-based method is preferable to the EKF algorithm if more than a couple of targets are to be tracked simultaneously, in both the 2D and 3D case.

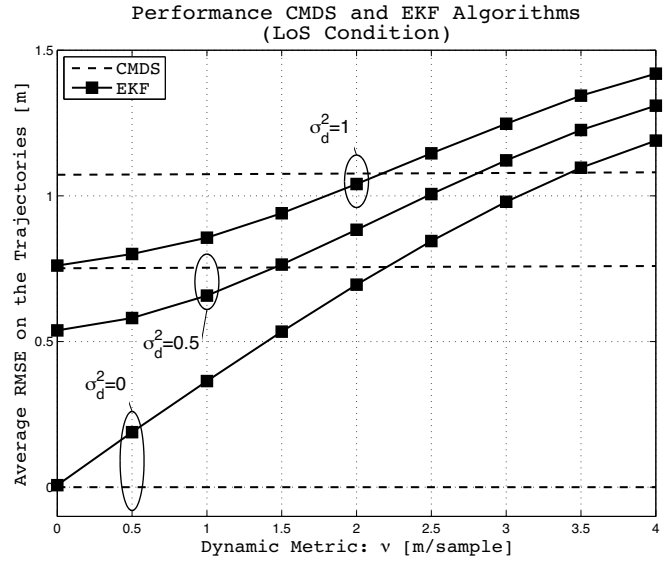
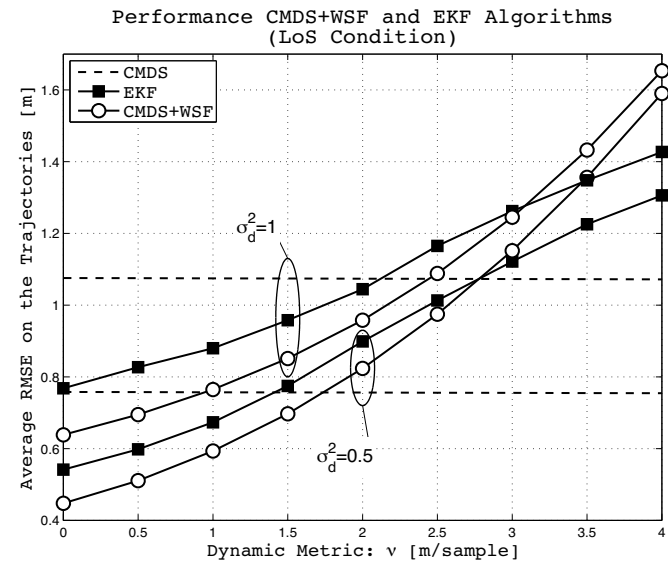

 (a) Algorithms performance in LoS as function of \bar{v} .

 (b) CMDS+WSF performance as function of \bar{v} .

 Fig. 3. Performance of the MDS and EKF tracking algorithms as a function of \bar{v} under perfect and noisy ranging.

In particular, in the 3D case, it can be noticed how the computational complexity required to track 50 targets with the CMDS+WSF method, allows to track less than half the same number of targets with the EKF algorithm. This, together with what already discussed in relation to the error-performance makes us to restrict the study for the NLoS case to the CMDS+WSF-based tracking solution only.

Figure 6 represents WSF filtering effect in case of ranging subject to equation (2), with the LoS-NLoS transition driven by the Markov Model described in II. The utility of WSF in detecting and mitigating the NLoS states is evident comparing the result for the observed data against the smoothed and the filtered one. In figure 6 the smoothed data are obtained employing the low-pass filter capability included in the wavelet transforms.

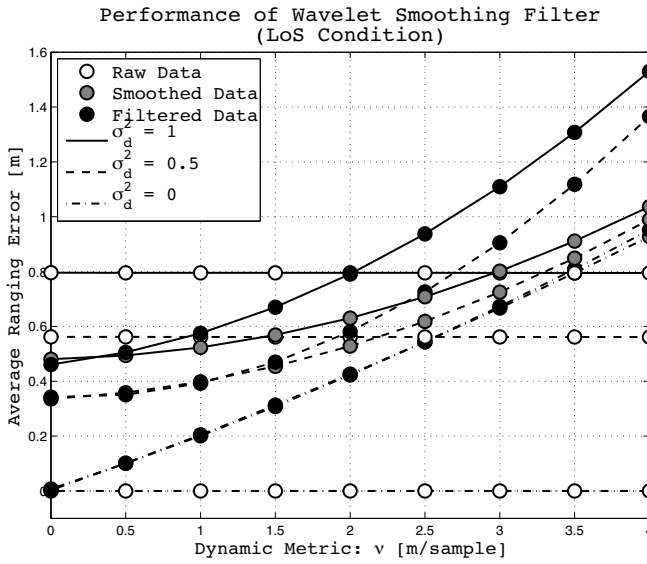


Fig. 4. WSF effect on corrupted measurements under mixed LoS condition for 3 different level of noise ($\sigma_d^2 = 0 - \sigma_d^2 = 0.5 - \sigma_d^2 = 1$).

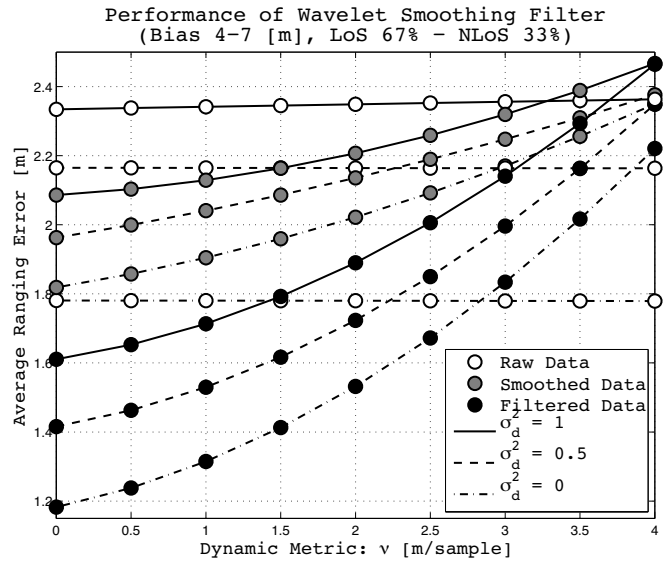


Fig. 6. WSF effect on corrupted measurements under mixed LoS-NLoS condition for 3 different level of noise ($\sigma_d^2 = 0 - \sigma_d^2 = 0.5 - \sigma_d^2 = 1$).

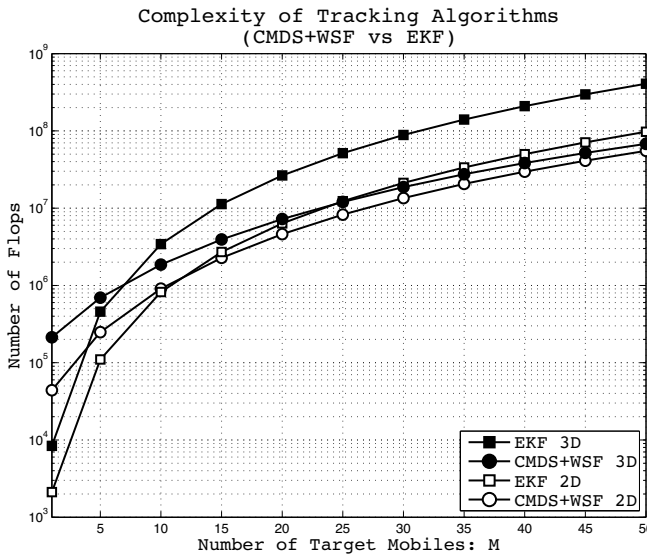


Fig. 5. Complexity of tracking Algorithms (EKF - CMDS+WSF) as a function of the number of targets in the case of both 2D-3D scenarios.

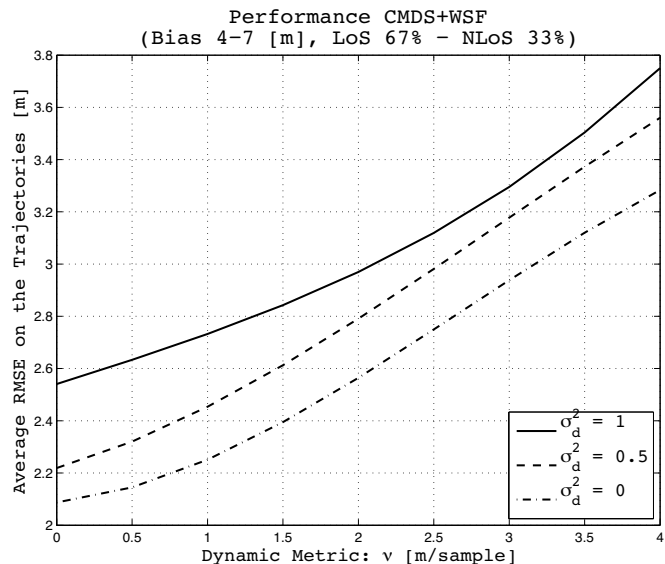


Fig. 7. CMDS+WSF performance under mixed LoS-NLoS conditions as function of \bar{v} under perfect and noisy ranging ($\sigma_d^2 = 0 - \sigma_d^2 = 0.5 - \sigma_d^2 = 1$).

Due to the permanence of the NLoS state and its occurrence, as described in II, the smoothing filter alone does not provide an adequate improvement to the range measurements. Instead, exploiting the capability for the WLS to simultaneously smooth and detect-mitigate the NLoS state affecting the observations, as described in III, it is possible to improve the quality of the observations without being strongly dependent on the dynamic \bar{v} .

The performance of the CMDS+WSF-based tracking algorithms under mixed LoS-NLoS for is shown in figure 7, for different σ_d^2 and with a bias generated as uniformly distributed between [4 – 7] meters.

The main conclusion of our study is that a subspace-based tracking algorithms (CMDS), together with the *pre*-filtering strategy here suggested (WSF), is advantageous, for the LoS case, under both complexity and error performance points of view, compared to EKF-based methods. In addition it allows to detect-mitigate biases in NLoS cases by the introduction of a small lag on the received observation and a very small additional computation complexity to on the tracking strategy.

VI. ACKNOWLEDGMENT

We would like to thank the European Project PULSERS phase II for sponsoring this work.

REFERENCES

- [1] T. Vercauteren, D. Guo, and X. Wang, "Joint multiple target tracking and classification in collaborative sensor networks," *IEEE J. Select. Areas Commun.*, vol. 23, no. 4, pp. 712–723, Apr. 2005.
- [2] M. Rydström, A. Urruela, E. Ström, and A. Svensson, "Low complexity tracking for ad-hoc automotive sensor networks," in *Proc. IEEE First Annual Communications Society Conference on Sensor and Ad Hoc Communications and Networks*, Oct. 4 - 7 2004, pp. 585 – 591.
- [3] R. Olfati-Saber and J. S. Shamma, "Consensus filters for sensor networks and distributed sensor fusion," in *Proc. IEEE Conference on Decision and Control - European Control Conference*, Dec. 12-15 2005, pp. 6698 – 6703.
- [4] D. Macagnano and G. Abreu, "Tracking multiple dynamic targets with multidimensional scaling," in *Proc. IEEE Personal Indoor Mobile Radio Communication*, Sept.3-7 2007.
- [5] D. Macagnano and G. T. F. de Abreu, "Tracking multiple targets with multidimensional scaling," in *Wireless Personal Multimedia Communications*, San Diego, U.S.A., Sep. 17 - 20 2006.
- [6] S.Mallat and S.Zhong, "Characterization of signals from multiscale edges," *IEEE Trans. Pattern Anal. Machine Intell.*, vol. 14, no. 7, pp. 710–732, July 1992.
- [7] G. Destino and G. Abreu, "Mds - wls optimization for sensors localization," in *IST*, June. 4 - 8 2006.
- [8] M.Rydstrom, M.Heidary, and K.Pahlavan, "A model for dynamic behaviour of ranging errors in toa-based indoor geolocation systems," in *IEEE Vehicular Technology Conference*, Sept. 2006.
- [9] O.Rioul and M.Vetterli, "Wavelets and signal processing," *IEEE Signal Processing Mag.*, October 1991.
- [10] S.Mallat, *A Wavelet Tour of Signal Processing*, 2nd ed. Academic Press, 1998.
- [11] —, "Multifrequency channel decompositions of images and wavelets models," *IEEE Trans. Acoustics. Speech. and Signal Processing*, vol. 37, no. 12, pp. 2091–2110, December 1989.
- [12] J. C. Platt, "Fastmap, metricmap, and landmark mds are all nystrom algorithms," Microsoft Research Technical Report, Tech. Rep. MSR-TR-2004-26, 2004. [Online]. Available: <http://citeseer.ist.psu.edu/732858.html>
- [13] J. Dattorro, *Convex Optimization and Euclidean Distance Geometry*. Meboo Publishing, 2005. [Online]. Available: <http://www.stanford.edu/~dattorro/mybook.html>
- [14] P. D. Fiore, "Efficient linear solution of exterior orientation," *IEEE Trans. Pattern Anal. Machine Intell.*, vol. 23, no. 2, pp. 140 – 148, February 2001.
- [15] G. H. Golub and C. F. van Loan, *Matrix Computations*, 3rd ed. New York, NY: Johns Hopkins Univ. Press, Nov. 1996.
- [16] A. Bunse-Gerstner, R. Byers, and V. Mehrmann, "Numerical methods for simultaneous diagonalization," *SIAM Journal on Matrix Analysis and Applications*, vol. 14, no. 4, pp. 927 – 949, 1993.
- [17] J.-F. Cardoso and A. Souloumiac, "Jacobi angles for simultaneous diagonalization," *SIAM Journal on Matrix Analysis and Applications*, vol. 17, no. 1, pp. 161 – 164, 1996.